

Article

Evidence for Vacancy Creation by Chromium Doping of Rutile Titanium Dioxide (110)

Ralf Bechstein, Mitsunori Kitta, Jens Schütte, Angelika Kühnle, and Hiroshi Onishi

J. Phys. Chem. C, **2009**, 113 (8), 3277-3280 • DOI: 10.1021/jp8095677 • Publication Date (Web): 04 February 2009

Downloaded from <http://pubs.acs.org> on February 20, 2009

More About This Article

Additional resources and features associated with this article are available within the HTML version:

- Supporting Information
- Access to high resolution figures
- Links to articles and content related to this article
- Copyright permission to reproduce figures and/or text from this article

[View the Full Text HTML](#)

Evidence for Vacancy Creation by Chromium Doping of Rutile Titanium Dioxide (110)

Ralf Bechstein,[†] Mitsunori Kitta,^{‡,§} Jens Schütte,[†] Angelika Kühnle,^{*,†} and Hiroshi Onishi[‡]

Fachbereich Physik, University of Osnabrueck, Barbarastrasse 7, 49076 Osnabrueck, Germany, and
Department of Chemistry, Kobe University, Rokko-dai, Nada-ku, Kobe 657-8501, Japan

Received: October 29, 2008; Revised Manuscript Received: December 19, 2008

Chromium doped rutile TiO₂(110) is studied using noncontact atomic force microscopy (NC-AFM) at room temperature. High-resolution NC-AFM images allow for investigating the effect of chromium doping on the surface structure at the atomic level. Besides added rows that are ascribed to Cr₂O₃ structures, we observe a considerable amount of surface hydroxyl defects, which are known to originate from oxygen vacancies. A careful analysis of the surface oxygen vacancy density is presented, providing strong experimental evidence for enhanced formation of surface oxygen vacancies upon chromium doping. We can explain these experimental results by a simple model based on maintaining charge neutrality while at the same time minimizing lattice stress. This simple model accounts for an increased oxygen vacancy density, in good agreement with our experimental findings.

1. Introduction

Photocatalysts find possible applications in the degradation of toxic compounds¹ and in the production of hydrogen fuel^{2–4} free from CO₂ release when driven by solar light. Doping with a foreign element is a promising method to sensitize a wide bandgap photocatalyst, e.g., TiO₂, with visible light.⁵ Nonmetallic dopants including carbon,⁶ nitrogen,⁷ fluorine,⁸ phosphorus,⁹ and sulfur¹⁰ have been examined and found to be active in visible-light induced reactions. Despite the successful sensitization, the nature of visible-light absorption sites is still under discussion. Band-gap narrowing,⁷ electronic transition from midgap states localized on dopants,^{8,11} and formation of oxygen anion vacancies as color centers^{12,13} are proposed to induce the visible-light absorption. Doping with transition metals often provides visible-light absorption more intense than with non-metal dopants.¹⁴ The formation of oxygen vacancies is again proposed with doping transition metals. For example, Cr³⁺ dopants are examined in TiO₂ along this scheme of sensitization. With Cr³⁺ dopants substituted for Ti⁴⁺ cations, oxygen anion vacancies appear to balance the ionic charges in the doped TiO₂.² Another particular interest in Cr-doped TiO₂ is ferromagnetism.¹⁵ On the other hand, experimental evidence for the dopant-induced formation of oxygen anion vacancies has not been provided. X-ray photoelectron emission and electron spin resonance are commonly used to know the oxidation state of dopants and Ti cations in the host crystals. The formation of oxygen vacancies is not directly evidenced, though this is sometimes related to the observed shift of oxidation states. Dilute dopants and oxygen vacancies, if any, appear in TiO₂ crystals without a long-range order. It is thus difficult to apply a reciprocal-space method like X-ray diffraction. Scanning probe microscopes are feasible to real-space imaging. Oxygen anion vacancies have been identified with scanning tunneling microscopes (STM)¹⁶ and NC-AFM¹⁷ on pristine TiO₂ surfaces. In an early STM study,¹⁸ branched structures were found on Cr-doped anatase TiO₂ films and

related with the Cr-induced lattice strain. On N-doped rutile samples, the enhanced formation stripe structures were observed when annealed in a vacuum and related to oxygen deficient composition of the doped sample.¹⁹ In the current study, a rutile TiO₂(110) sample was doped with chromium and investigated by NC-AFM. Our results constitute strong experimental evidence for enhanced surface oxygen vacancy formation upon chromium doping of rutile titania.

2. Experimental Section

In this study, we use NC-AFM operated in the frequency modulation mode. For this technique, a sharp nanoscopic tip mounted at the end of an oscillating cantilever is scanned in close proximity over the sample surface while keeping the oscillation amplitude constant. The forces acting between tip and surface atoms shift the cantilever's eigenfrequency. This frequency shift can be directly used as an imaging signal when scanning the cantilever at a fixed tip–surface distance (constant height mode). Alternatively, the frequency shift can be kept constant to measure the height profile of equal frequency shift (referred to as topography). Measurements are performed in an ultrahigh vacuum (UHV) chamber (base pressure below 10^{−10} mbar) equipped with a VT AFM 25 (Omicron, Taunusstein, Germany) and an easy-PLL Plus phase-locked loop controller (Nanosurf, Liestal, Switzerland) for oscillation excitation and signal demodulation. We use silicon cantilevers (type PPP-NCH) from NanoWorld (Neuchâtel, Switzerland) with a resonance frequency of about 300 kHz operated at an amplitude of 10 nm. For these experiments, the cantilevers are sputtered with Ar⁺ ions after insertion into the chamber. The TiO₂ samples are crystals of highest quality available (MTI, Richmond, USA). The crystals were doped with chromium by calcining them together with Cr₂O₃ powder in a crucible at 1420 K for 10 h in air. The total amount of chromium in the doped crystal is difficult to quantify; however, in the upper few micrometers, the chromium concentration is known to be on the order of 2–3 atom percent.^{20,21} After insertion into the UHV chamber, the surface was cleaned by cycles of Ar⁺ ion sputtering at 1 keV and annealing at 1100 K. The preparation parameter were chosen in accordance with our experience on pristine TiO₂. In order to

* To whom correspondence should be addressed. E-mail: kuehnle@uos.de.

[†] University of Osnabrueck.

[‡] Kobe University.

[§] Present address: Department of Chemistry, School of Science, Osaka University, Mihogaoka, Ibaraki, Osaka, 567-0047 Japan.

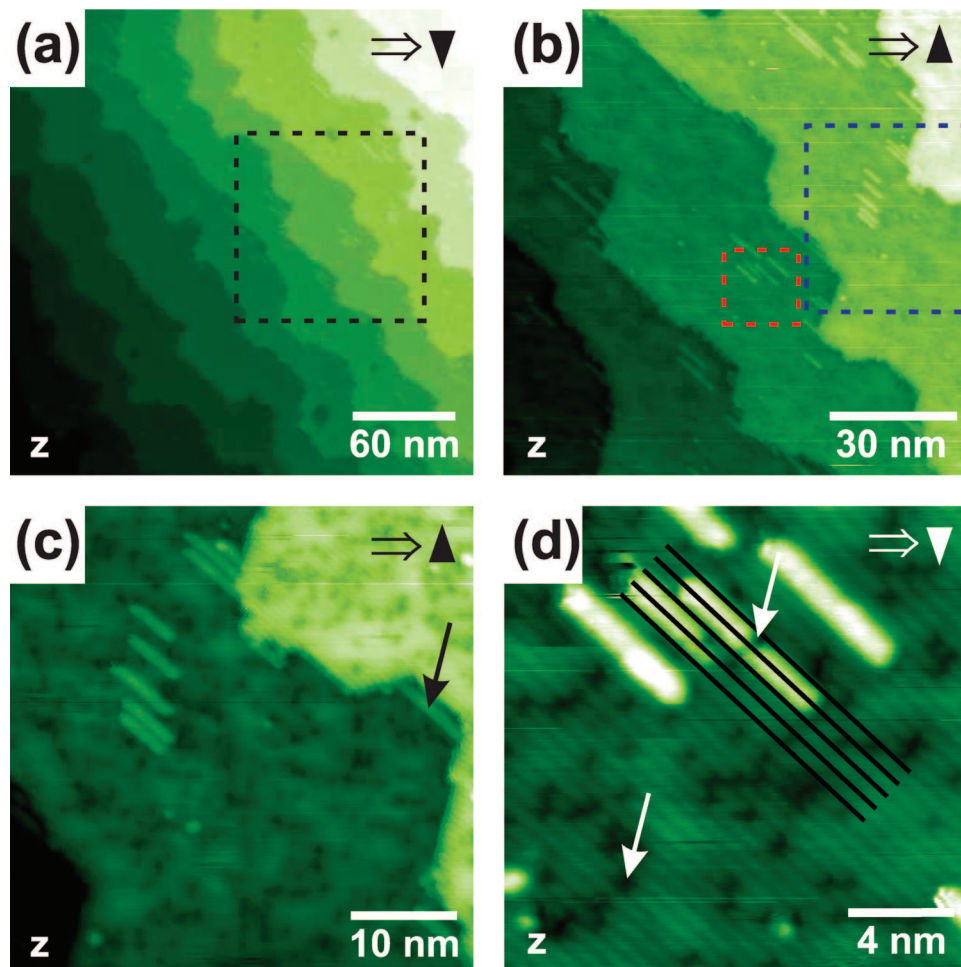


Figure 1. Subsequently taken topography images of chromium-doped TiO_2 . (a) Overview image showing the stepped surface. The step height is (3.4 ± 0.3) Å. (b) All stripes are aligned in the [001] direction. (c) Some stripes are growing from step edges, or even connect them (black arrow), however, the majority of stripes is found on the terraces. (d) A large number of hydroxyls can be identified as dark features in bright oxygen rows. Two of them are indicated by white arrows; one interrupting a stripe feature and one on the bare terrace. The stripes are centered on titanium rows.

minimize long-range electrostatic interactions, a bias voltage of about -1.6 V was applied to the tip.

3. Results and Discussion

Our main interest in this study was to investigate the influence of chromium doping on the surface structure of TiO_2 . Figure 1 shows a series of topography images recorded subsequently upon decreasing the frame size. At large frame size (Figure 1a) the typical appearance of pristine $\text{TiO}_2(110)$ is observed. The step height was measured to be (3.4 ± 0.3) Å which is very similar to that of undoped titanium dioxide [3.25 Å]. Besides the typical $\text{TiO}_2(110)$ appearance, a number of additional stripes can be identified (Figure 1b). These stripes are exclusively aligned along the [001] direction and observed to have a length of 5–10 nm. Although few stripes grow from step edges the majority of the stripes are found on the terraces.

At small frame sizes (Figure 1c), the substrate atoms become visible as bright rows. These rows are disrupted by dark features originating from atomic-size defects (Figure 1d). This contrast mode has been reported before and referred to as hole mode.²² Based on this assignment, we can identify the bright rows as bridging oxygen atoms, the dark rows as titanium atoms, and the dark defects in the bright rows as hydroxyls. The distance of the oxygen rows was measured to be (6.3 ± 0.2) Å. Within the error, this corresponds to the lattice distance of $\text{TiO}_2(110)$ [6.5 Å].

From Figure 1d, it is obvious that the bright stripes are always centered on titanium rows overlapping the neighboring oxygen rows. One probable explanation for the stripes could be that they consist of reduced titania Ti_2O_3 as observed on samples that have been annealed at higher temperatures.²³ These Ti_2O_3 rows have been reported to be precursors of the (1×2) reconstructed surface. Although the appearance of our stripes is very similar to the known Ti_2O_3 rows, three strong arguments exist against this assumption. First of all, the annealing temperature in these experiments was exactly the same as in our previous experiments on pristine titania, which never resulted in the formation of reduced Ti_2O_3 rows. Second, when reducing the tip-sample distance to obtain better resolution, it was often observed that the stripe features were moved on the substrate. This fact points toward a rather weak interaction of the stripes with the substrate, in contrast to what is expected for Ti_2O_3 rows. Third, the fact that the density of stripes is reduced upon further preparation is the strongest argument against the assignment of the rows being Ti_2O_3 . Titanium dioxide is known to become slightly reduced by sputtering and annealing under vacuum conditions. Further reduction would lead to an increasing amount of material consisting of reduced titania, eventually resulting in a (1×2) reconstructed surface. In contrast, in our experiment, the number of stripe features on the doped surface is observed to be massively reduced by

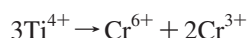
TABLE 1: Ionic Radii of Metal Ions Taken from Shannon (1976)²⁶

cation	ionic radius (pm)
Ti ³⁺	67.0
Ti ⁴⁺	60.5
Cr ³⁺	61.5
Cr ⁶⁺	44.0

repeated preparation. We will find that these stripes most likely consist of Cr₂O₃ as discussed later.

We will now take a detailed look at the density of the dark holes within the bright oxygen rows, which can be assigned to single hydroxyl defects. These hydroxyls are known to evolve from oxygen vacancies. From one oxygen vacancy, two hydroxyls are created upon water adsorption.²⁴ As indicated in Figure 1d the hydroxyls are observed to be homogeneously distributed. From a statistical analysis we quantified the density of hydroxyls to be $(4.9 \pm 0.6)\%$ ML after seven cycles of sputtering and annealing (100% ML corresponds to one hydroxyl per surface unit cell). As two hydroxyls are formed from one oxygen vacancy, the measured hydroxyl density corresponds to an initial oxygen vacancy density of $(2.45 \pm 0.30)\%$ ML. We can now compare this value to what we usually observe on undoped TiO₂(110). From an extended defect density study in dependence on preparation duration accomplished on pristine titanium, we expect a vacancy density on the order of $(0.45 \pm 0.30)\%$ ML after seven cycles of preparation.²⁵ Thus, in the present experiments, the vacancy density is strikingly larger than commonly observed on pristine TiO₂(110). Even when considering the rather large error bars of the density measurement, the present vacancy density remains to be at least 1.40% ML too high. Thus, the additional defects cannot be explained by the sample preparation procedure, but must be associated with the calcination process. Note that calcination in air during the doping procedure does not per default reduce the bulk as indicated by the transparent appearance of a similarly treated antimony-doped titania sample (not shown). Hence, the total amount of additional vacancies must be exclusively induced by the presence of chromium dopant.

Before we present our model that explains the reason for the creation of extra oxygen vacancies during the calcination process, we need to remember the oxidation state of chromium dopants in chromium-doped TiO₂. The oxidation state of chromium is most likely either Cr³⁺ or Cr⁶⁺. Chromium atoms replace Ti⁴⁺ in the titanium dioxide bulk. If only Cr³⁺ or Cr⁶⁺ exists solely in the doped sample, the crystal would be negatively or positively charged, respectively. Hence, the oxidation state of chromium is heterogeneous in chromium-doped TiO₂.²¹ Charging could be easily avoided (without the creation of oxygen vacancies) as illustrated by



This formula indicates that one out of three chromium atoms replacing titanium atoms needs to be in Cr⁶⁺ state for maintaining charge neutrality. The other two chromium atoms are in the oxidation state Cr³⁺. As the sum of oxidation states is equal $(3 \times 4 = 6 + 2 \times 3)$ before and after the replacement, the crystal remains uncharged upon doping.

Nevertheless, charge compensation is only one requirement for crystal stability. Another very important issue is minimization of stress due to lattice mismatch. For the situation illustrated above, a mean ionic radius of 55.7 pm can be estimated for the three chromium dopants (see ionic radii given in Table 1). The dopants replace Ti⁴⁺ with an ionic radius of 60.5 pm, resulting

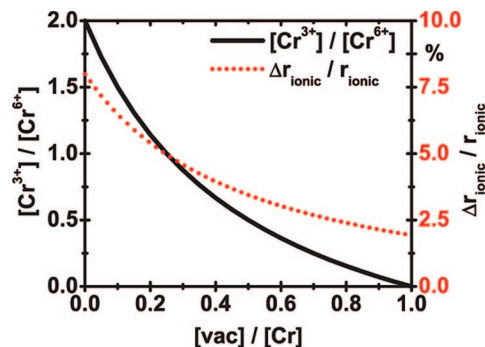
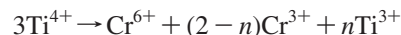


Figure 2. (color online) Ratio of the chromium atoms of different oxidation state Cr³⁺:Cr⁶⁺ (black, solid line) and mean ionic radius mismatch (red, dotted line) in dependence on the [vac]:[Cr] ratio. The whole range of possible mixtures maintaining charge neutrality is shown.

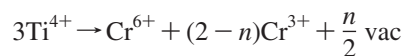
in a mean ionic radius mismatch of about 8%. Even if these numbers must not be taken too literally, this model does, indeed, indicate that the situation above might be unfavorable although the charge is fully compensated.

It can directly be seen from Table 1 that the ionic radii of Cr³⁺ and Ti⁴⁺ are very similar. Hence, the lattice mismatch results from the fact that the ionic radius of Cr⁶⁺ is much smaller than that of Ti⁴⁺. To compensate for this small ionic radius, a species with an ionic radius larger than that of Ti⁴⁺ is needed. Obviously, Ti³⁺ is such a candidate. Considering the creation of Ti³⁺ during the calcination process, the formula introduced above has to be modified as follows to maintain charge neutrality



where $n \in [0, 2]$. This formula shows that Ti³⁺ instead of Cr³⁺ or a mixture could be responsible for charge compensation, provided that Ti³⁺ can be formed by charge redistribution.

In the surface layer, Ti³⁺ can be also created by loss of oxygen. A single oxygen vacancy is created by the loss of a neutral oxygen atom, reducing the two adjacent titanium atoms from Ti⁴⁺ to Ti³⁺ state. As these two Ti³⁺ are intrinsically tied to one vacancy, $n\text{Ti}^{3+}$ in the preceding formula represents $n/2$ vacancies (vac) in the surface layer. Thus, one ends up with



The mean ionic radius mismatch of this situation can be estimated according to the values from Table 1 as a function of the parameter n . The result is given in Figure 2. To be more illustrative, we do not plot the ionic radius mismatch against n itself but against the ratio of vacancy density to chromium density $[\text{vac}]:[\text{Cr}] = n/2(3 - n) \in [0, 1]$. At a given n , also the ratio $[\text{Cr}^{3+}]:[\text{Cr}^{6+}] = (2 - n)$ is a fixed value for maintaining charge neutrality. This curve is also given in Figure 2. Now, two extreme situations can be distinguished: $n = 0$ (no Ti³⁺) and $n = 2$ (no Cr³⁺). It is obvious from Figure 2 that the mismatch is maximal (approximately 8%) in the absence of Ti³⁺, showing that this is the most unlikely situation. Lattice stress will be reduced by increasing the amount of Ti³⁺, but as a result the amount of Cr³⁺ decreases to maintain charge neutrality. This simple model would predict that all chromium atoms should be in the 6+ state for minimizing the lattice stress, although we know from spectroscopy that this is not the case.²¹ This discrepancy might occur, as we did not consider the implications of the resulting bulk reduction of as high as 10% on the crystal stability in our simple model. Still, this model indicates why additional oxygen vacancies are created during the calcination

process. Moreover, our model allows for giving a rough estimation for the vacancy concentration. Assuming a tolerable lattice mismatch of 3% at highest, the proposition from the model is that the concentration of vacancies should be of the same order of magnitude as the total amount of chromium ($[\text{vac}]:[\text{Cr}] \geq 0.5$ equivalent to $n \geq 1.5$).

Interestingly, the prediction of our simple model exactly matches the findings of our experiment. While the total amount of chromium is expected to be on the order of 2–3 atom percent (at least in the upper few layers), we found the vacancy density of the freshly doped sample to be at least 1.4% ML. This gives a ratio $[\text{vac}]:[\text{Cr}]$ of more than 0.5, as predicted by our model.

However, the strongest hint for the correctness of our model is the fact that we do not see an enhanced density of oxygen vacancies on the surface of $\text{TiO}_2(110)$ doped with chromium and antimony at a ratio of about unity (not shown). In this sample the charge neutrality is provided by an equal amount of Cr^{3+} and Sb^{5+} . The ionic radii of these ions are 61.5 and 60.0 pm, respectively.²⁶ Both are very close to the radius of Ti^{4+} resulting in virtually no mismatch. Eventually charge redistribution to titanium is not necessary; therefore, no additional oxygen vacancies are found on this surface.

Assuming this model to be correct, what happens if the sample is prepared in UHV? Sputtering and annealing under UHV conditions is known to reduce titanium dioxide,²⁴ which leads to an even higher oxygen vacancy concentration. To maintain charge neutrality, an equal amount of Cr^{3+} has to leave the bulk, restoring the ratio $([\text{Cr}^{3+}] + [\text{Ti}^{3+}]):[\text{Cr}^{6+}] = 2$. This explains why Cr_2O_3 features are found on the surface. These Cr_2O_3 stripes are favorably sputtered during the following cycles. Consequently, two parallel processes are taking place at the same time. First, we increase the density of oxygen vacancies by sputtering and annealing (we already reached a vacancy concentration of 2.45% ML in our experiment). Second, as a direct result, we decrease the amount of chromium during following sputtering cycles, as we remove Cr_2O_3 from the surface. Both processes will lead to the situation where the density of vacancies and the density of chromium dopants near the surface is equal ($[\text{vac}]:[\text{Cr}] = 1$). Hence, all chromium atoms in the upper bulk layers will be in the 6+ state. At this point segregation of Cr^{3+} to the surface stops and following preparation cycles will remove the remaining Cr_2O_3 . This explains why the density of Cr_2O_3 stripes decreases upon further preparation.

4. Conclusions

We have investigated the (110) surface of rutile TiO_2 doped with 2–3 atom percent chromium by NC-AFM. The surface lattice parameters were observed to be very similar to that of pristine titanium dioxide. Nevertheless, two main differences have been observed. First, a number of stripe-like features centered on top of titanium rows and aligned in the [001] direction were found. These stripes can be assigned to Cr_2O_3 that evolves from Cr^{3+} segregating to the surface as a direct result from bulk reduction by UHV preparation. Second, the density of oxygen vacancies was found to be drastically

increased compared to pristine TiO_2 , indicating that oxygen vacancies are created during the calcination process. We present a simple model that accounts for these experimental findings. The model is based on reducing lattice stress while maintaining charge neutrality at the same time. As a result, only a minority of chromium atoms in chromium-doped TiO_2 can be in the 3+ state. It has to be discussed whether this fact is also responsible for the lack of photocatalytic activity of chromium-doped titanium dioxide.

Acknowledgment. Financial support from the Deutsche Forschungsgemeinschaft (DFG) through an Emmy Noether grant is gratefully acknowledged.

References and Notes

- (1) Fujishima, A.; Rao, T. N.; Tryk, D. A. *J. Photochem. Photobiol. C* **2000**, *1*, 1–21.
- (2) Kudo, A.; Niishiro, R.; Iwase, A.; Kato, H. *Chem. Phys.* **2007**, *339*, 104–110.
- (3) Kato, H.; Kudo, A. *Catal. Today* **2003**, *78*, 561–569.
- (4) Maeda, K.; Teramura, K.; Lu, D. L.; Takata, T.; Saito, N.; Inoue, Y.; Domen, K. *Nature* **2006**, *440*, 295.
- (5) Chen, X.; Mao, S. S. *Chem. Rev.* **2007**, *107*, 2891–2959.
- (6) Irie, H.; Watanabe, Y.; Hashimoto, K. *Chem. Lett.* **2003**, *32*, 772–773.
- (7) Asahi, R.; Morikawa, T.; Ohwaki, T.; Aoki, K.; Taga, Y. *Science* **2001**, *293*, 269–271.
- (8) Czoska, A. M.; Livraghi, S.; Chiesa, M.; Giamello, E.; Agnoli, S.; Granozzi, G.; Finazzi, E.; Di Valentin, C.; Pacchioni, G. *J. Phys. Chem. C* **2008**, *112*, 8951–8956.
- (9) Lin, L.; Lin, W.; Zhu, Y.; Zhao, B.; Xie, Y. *Chem. Lett.* **2005**, *34*, 284–285.
- (10) Ohno, T.; Mitsui, T.; Matsumura, M. *Chem. Lett.* **2003**, *32*, 364–365.
- (11) Diwald, O.; Thompson, T. L.; Zubkov, T.; Goralski, E. G.; Walck, S. D.; Yates, J. T., Jr. *J. Phys. Chem. B* **2004**, *108*, 6004–6008.
- (12) Serpone, N. *J. Phys. Chem. B* **2006**, *110*, 24287–24293.
- (13) Livraghi, S.; Paganini, M. C.; Giamello, E.; Selloni, A.; Di Valentin, C.; Pacchioni, G. *J. Am. Chem. Soc.* **2006**, *128*, 15666–15671.
- (14) Di Paola, A.; Marci, G.; Palmisano, L.; Schiavello, M.; Uosaki, K.; Ikeda, S.; Ohtani, B. *J. Phys. Chem. B* **2002**, *106*, 637–645.
- (15) Kaspar, T. C.; Droubay, T.; Shuttanandan, V.; Heald, S. M.; Wang, C. M.; McCready, D. E.; Thevuthasan, S.; Bryan, J. D.; Gamelin, D. R.; Kellock, A. J.; Toney, M. F.; Hong, X.; Ahn, C. H.; Chambers, S. A. *Phys. Rev. B* **2006**, *73*, 155327.
- (16) Diebold, U. *Surf. Sci. Rep.* **2003**, *48*, 53–229.
- (17) Fukui, K.-I.; Onishi, H.; Iwasawa, Y. *Phys. Rev. Lett.* **1997**, *79*, 4202–4205.
- (18) Ohsawa, T.; Yamamoto, Y.; Sumiya, M.; Matsumoto, Y.; Koinuma, H. *Langmuir* **2004**, *20*, 3018–3020.
- (19) Batzill, M.; Morales, E. H.; Diebold, U. *Phys. Rev. Lett.* **2006**, *96*, 026103.
- (20) Kato, H.; Kudo, A. *J. Phys. Chem. B* **2002**, *106*, 5029–5034.
- (21) Ikeda, T.; Nomoto, T.; Eda, K.; Mizutani, Y.; Kato, H.; Kudo, A.; Onishi, H. *J. Phys. Chem. C* **2008**, *112*, 1167–1173.
- (22) Lauritsen, J. V.; Foster, A. S.; Olesen, G. H.; Christensen, M. C.; Kühnle, A.; Helveg, S.; Rostrup-Nielsen, J. R.; Clausen, B. S.; Reichling, M.; Besenbacher, F. *Nanotechnology* **2006**, *17*, 3436–3441.
- (23) Onishi, H.; Iwasawa, Y. *Surf. Sci.* **1994**, *313*, L783–L789.
- (24) Wendt, S.; Schaub, R.; Matthies, J.; Vestergaard, E. K.; Wahlstroem, E.; Rasmussen, M. D.; Thostrup, P.; Molina, L. M.; Laegsgaard, E.; Stensgaard, I.; Hammer, B.; Besenbacher, F. *Surf. Sci.* **2005**, *598*, 226–245.
- (25) Schütte, J.; Bechstein, R.; Rahe, P.; Langhals, H.; Rohlfling, M.; Kühnle, A. *Phys. Rev. B* **2008**, accepted.
- (26) Shannon, R. D. *Acta Crystallogr., Sec. A* **1976**, *32*, 751–767.